Journal of
Applied Remote Sensing

RemoteSensing.SPIEDigitalLibrary.org

Introducing the geostationary environment monitoring spectrometer

Won Jun Choi
Kyung-Jung Moon
Jongmin Yoon
Ara Cho
Sang-kyun Kim
Seounghoon Lee
Dai ho Ko
Jhoon Kim
Myung Hwan Ahn
Deok-Rae Kim
Sang-Min Kim
Ji-Young Kim
Dennis Nicks
Jeong-Su Kim

SPIE.

Won Jun Choi, Kyung-Jung Moon, Jongmin Yoon, Ara Cho, Sang-kyun Kim, Seounghoon Lee, Dai ho Ko, Jhoon Kim, Myung Hwan Ahn, Deok-Rae Kim, Sang-Min Kim, Ji-Young Kim, Dennis Nicks, Jeong-Su Kim, "Introducing the geostationary environment monitoring spectrometer," *J. Appl. Remote Sens.* **12**(4), 044005 (2019), doi: 10.1117/1.JRS.12.044005.

Introducing the geostationary environment monitoring spectrometer

Won Jun Choi,[a,c] Kyung-Jung Moon,[a] Jongmin Yoon,[a,*] Ara Cho,[a] Sang-kyun Kim,[a] Seounghoon Lee,[b] Dai ho Ko,[b] Jhoon Kim,[c] Myung Hwan Ahn,[d] Deok-Rae Kim,[a] Sang-Min Kim,[a] Ji-Young Kim,[a] Dennis Nicks,[e] and Jeong-Su Kim[a]

[a]National Institute of Environmental Research, Incheon, Republic of Korea
[b]Korea Aerospace Research Institute, Daejeon, Republic of Korea
[c]Yonsei University, Department of Atmospheric Sciences, Seoul, Republic of Korea
[d]Ewha Womans University, Seoul, Republic of Korea
[e]Ball Aerospace Technologies Corporation, Colorado, United States

Abstract. To consistently observe deteriorating air quality over East Asia, the National Institute of Environmental Research, Republic of Korea, is planning to launch an environmental observation sensor, the Geostationary Environment Monitoring Spectrometer (GEMS), onboard the GK-2B satellite (a successor to the GeoKOMPSAT-1) in late 2019. GEMS is a hyperspectral spectrometer that covers the ultraviolet–visible range (300 to 500 nm) with full-width at half-maximum of 0.6 nm. It has been designed for the observation of air pollutants and short-lived climate pollutants. GEMS captures images at hourly intervals in the daytime, alternating with the Geostationary Ocean Color Imager-II every 30 min. Over the Seoul Special Metropolitan area, South Korea, the spatial sampling resolution of GEMS is 3.5×8 km (north–south and east–west, respectively). There are 16 baseline products, including aerosol optical depth and the vertical column density of trace gases such as nitrogen dioxide, sulfur dioxide, formaldehyde, and ozone. Research continues into additional applications (e.g., ground-level concentrations and emissions). [DOI: 10.1117/1.JRS.12.044005]

Keywords: geostationary environmental satellite; remote sensing; air quality; atmospheric pollutant.

Paper 180804 received Oct. 9, 2018; accepted for publication Nov. 30, 2018; published online Dec. 27, 2018; corrected Dec. 31, 2018.

1 Introduction

Nearly three million premature deaths are attributed to air pollution each year;[1] ~90% of the world's population is in constant danger of exposure to high levels of particulate matter (PM) with an aerodynamic diameter ≤ 2.5 μm (PM2.5).[2] Due to various factors including ongoing industrialization and urbanization with significant changes in climate and geography, especially over East Asia, South Korea had the worst air quality among the Organization for Economic Co-operation and Development (OECD) nations in 2013. Averaged annual exposure to PM2.5 over 3 years (2010 to 2012) was 29.09 $\mu g/m^3$, significantly greater than the OECD mean of 14.05 $\mu g/m^3$.[3] In addition, PM10 levels (PM with a diameter ≤ 10 μm), which had been consistently improving since the 1990s, have deteriorated since 2013, while high concentrations of fine particles are becoming more common.

To address this deteriorating air quality, the South Korean government established the "Special Act on the Improvement of Air Quality in Seoul Metropolitan Area" and invested approximately $3 billion during phase 1 (2005 to 2014).[4] Policies regulating air pollutant emissions have resulted in significant reductions in sulfur oxides, nitrogen oxides, volatile organic compounds (VOCs), and PM10 (Table 1). However, the concentrations of nitrogen oxides and

*Address all correspondence to Jongmin Yoon, E-mail: ofjyoon@korea.kr

Table 1 Air quality conditions before and after phase 1 of the "Special Act on the Improvement of Air Quality in Seoul Metropolitan Area," and phase 2 goals.

Item	PM_{10}	$PM_{2.5}$ (goal)	NO_2	O_3 (goal)
2001	71 $\mu g/m^3$	—	37 ppb	—
2010	47 $\mu g/m^3$	27 $\mu g/m^3$	34 ppb	87 ppb
2024 (target)	30 $\mu g/m^3$	20 $\mu g/m^3$	21 ppb	60 ppb

PM2.5 remain high when compared with other developed nations.[5,6] Phase 2 is currently underway with a total budget projected to be approximately $4 billion over the next 10 years.

For air quality improvement policies to succeed, the relationships between sources and quantities of air pollutants in the atmosphere need to be more accurately understood. Moreover, optimum reduction quantities and efficient reduction scenarios require determination. Therefore, it is critical to distinguish between the contributions of domestic sources and foreign influxes to direct air quality improvement policies. Additionally, depending on climatic conditions, air pollutants emitted from surrounding nations directly impact the South Korean atmosphere with a lag time of 1 to 2 days.[7] For example, recent increases in air pollution over South Korea have been closely attributed to air pollutant emissions from China.[8–11] Therefore, multilateral and international efforts have been proposed to determine the effects of long-range air pollutant transport and thus to improve air quality in East Asia. These efforts include the launching of joint research groups between South Korea and China, the operation of long-range transboundary air pollutant (LTP) projects among South Korea, Japan, and China,[12,13] and discussions at the Tripartite Environment Ministers Meeting and Korea–United States Air Quality Campaign.[14,15]

The South Korean government is in the process of expanding its ground observation network used for monitoring air quality. It has also been performing episodic aerial monitoring to efficiently establish and enforce air quality policies, and to acquire fundamental scientific data. However, precise assessments are still limited due to deficient data from ground-based observations that do not sufficiently cover contiguous large target areas of interest. The development of advanced remote sensing technologies as well as the consistent monitoring of trace gases in the atmosphere directly contributes to overcoming these limitations, thereby improving our ability to analyze long-range transported air pollutants.[16] Currently operational low Earth orbit (LEO) environmental satellites[16–21] are capable of monitoring air quality on a global scale; however, they are temporally limited to observing the same location only every 1 to 3 days. To consistently monitor deteriorating air quality over East Asia, the National Institute of Environmental Research (NIER), Republic of Korea, is planning to launch a satellite-based environmental observation instrument, the Geostationary Environment Monitoring Spectrometer (GEMS), in late 2019. GEMS is expected to perform quantitative analyses on air pollution phenomena in the East Asian region.[22,23]

2 GEMS Mission Overview

GEMS development was initiated in 2012 along with an advanced ocean color imager, the Geostationary Ocean Color Imager-II (GOCI-II).[24] Both sensors will be launched onboard GeoKOMPSAT-2B (GK-2B) as part of the GK-2 mission, which consists of two satellites (GK-2A/B):[25] the 2A satellite, which carries the Advanced Meteorological Imager (AMI) for weather surveys, and the 2B satellite, which carries GOCI-II and GEMS for ocean and atmospheric environmental monitoring.

The AMI, GOCI-II, and GEMS sensors each have unique spectral and spatial coverage with resolutions optimized for their respective missions. In addition to the major products obtained from each payload, additional products are expected to be utilized by integrating the GK-2A/B observation data based on their different spectral and spatial resolutions. Research to develop potentially new output categories, and to improve the accuracy of existing outputs via the integration of payload data, is currently underway.

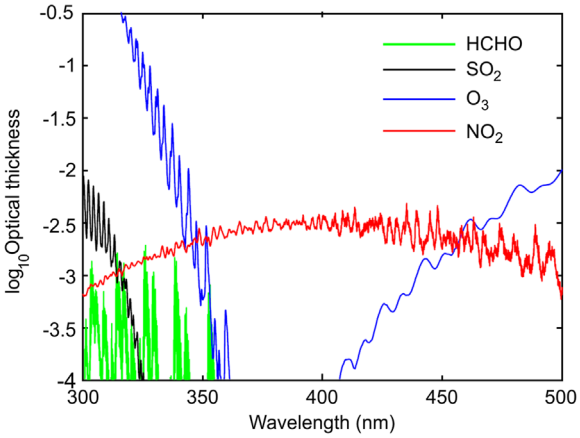

Fig. 1 Optical thickness of atmospheric species of interest as a function of wavelength. Adapted from Ref. 19.

GEMS is scheduled to be launched after October 2019. Along with the Tropospheric Emissions: Monitoring Pollution (TEMPO) of the United States' National Aeronautics and Space Administration (NASA), and Sentinel-4 of the European Space Agency (ESA), GEMS is expected be an essential part of the GEO air quality constellation for monitoring global air quality.[22,23]

2.1 *Spatial and Spectral Coverage*

The region of interest for GEMS covers East Asia, corresponding to longitudes 75° E–145° E and latitudes of 5° S–45° N. Its sampling spatial resolution is 3.5×8 km (north–south and east–west, respectively) per pixel at Seoul, with spatial and temporal co-adding depending on product category.

GEMS provides trace gas concentrations through a spectroscopic algorithm that calculates concentrations based on the gas absorption cross section with regards to solar irradiance (Fig. 1). The spectrometer observes ultraviolet–visible wavelengths in the 300- to 500-nm range with a sampling spectral resolution of 0.2 nm, and a full-width at half-maximum (FWHM) of 0.6 nm, which is the sum of all three spectral sampling data sources; thus its operation is limited to the daytime.

2.2 *Observation Modes*

GEMS and GOCI-II will operate alternatively every 30 min to capture hourly images; GEMS covers a wider area, from east of Japan to Indonesia (Fig. 2). Its operational scenario includes a concentrated observation mode that allows enhancement of its signal-to-noise ratio (SNR) by reducing the east–west scan range during the mornings and evenings when solar radiation is weak. GEMS can utilize three observational modes: normal observation, East Asia observation, and local area observation. These observational modes can be utilized to closely monitor corresponding areas during instances of high air pollution (Table 2).

3 Instrument Design and Performance

3.1 *Overall Design and Performance*

In normal mode, GEMS observes its field of view (FOV; Fig. 2) from east to west by moving its scan mirror position a total of 701 times. At a given scan position, 37 images over a period of 63.5 ms are coadded onboard to enhance its SNR; coadding is possible up to 63 times (Fig. 3). However, GEMS is limited to only 30 min of observation per hour, and its allowable FOV decreases for concentrated observations to enhance SNR. Earth radiance values are given as

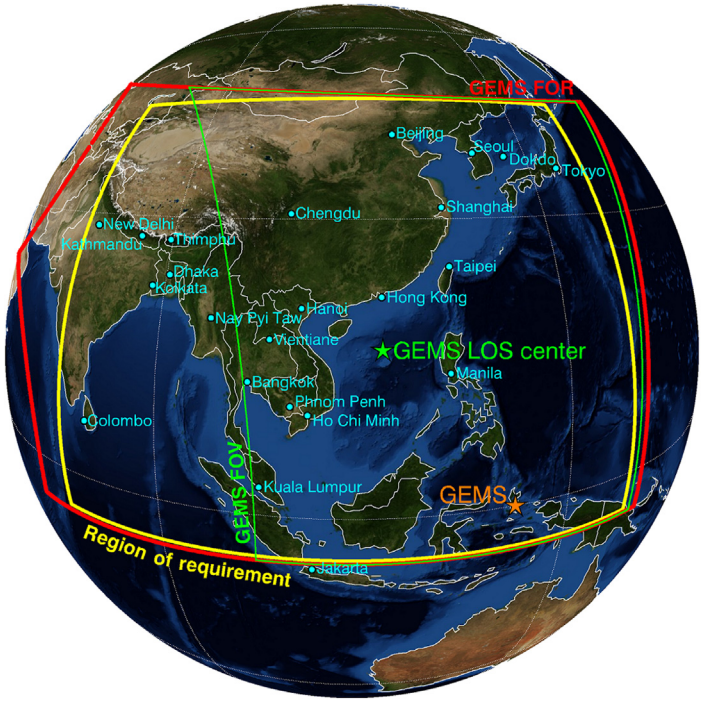

Fig. 2 Region of requirement (yellow box), GEMS field of regard (FOR) (red box), and GEMS FOV (green box) for the GEMS. The background satellite imagery data are obtained from the Blue MarbleNext Generation. (Image credit: Reto Stckli, NASA Earth Observatory.)

Table 2 Main features of the GEMS.

Operational observation modes		Observation cycle (min)	East–west scanning range (longitude based on Seoul)	Notes
General observation		60	75°E–145°E	
Special observation	East Asia (EA) mode	60	110°E–140°E	Monitoring of East Asian region
	Enhanced East Asia (EEA) mode	60	115°E–130°E	Enhanced monitoring of East Asian region
				Operational mode for winter
	Local area (LA) mode	30	Based on ground command	For emergency situations on the Korean Peninsula

$$P2_{i,j}(DN) = \sum_{k=1}^{k=CON} \{P1_{i,j}(DN)\}_k, \tag{1}$$

where i is the spectral position and j is the ground position (north-south direction); $P1_{i,j}(DN)$ is the focal plane subsystem output with 14 bits/pixel; $P2_{i,j}(DN)$ is the Earth observation radiance value; CON is the number of Earth observations (generally 37, maximum 63); and DN is the mirror position (generally 1 to 701).

The design of GEMS, including the light path, uses optical paths equal to those used in observing the Earth and Sun for spectral calibration (Fig. 4). The grating and reflector spectroscopic parts were designed in the form of an Offner relay to minimize distortion. One scan spatially covers 2048 pixels in a north–south direction (one pixel corresponds to 3.5 km at Seoul) and spectrally covers 1000 pixels (spectral resolution of 0.2 nm); scanned data are sent to ground

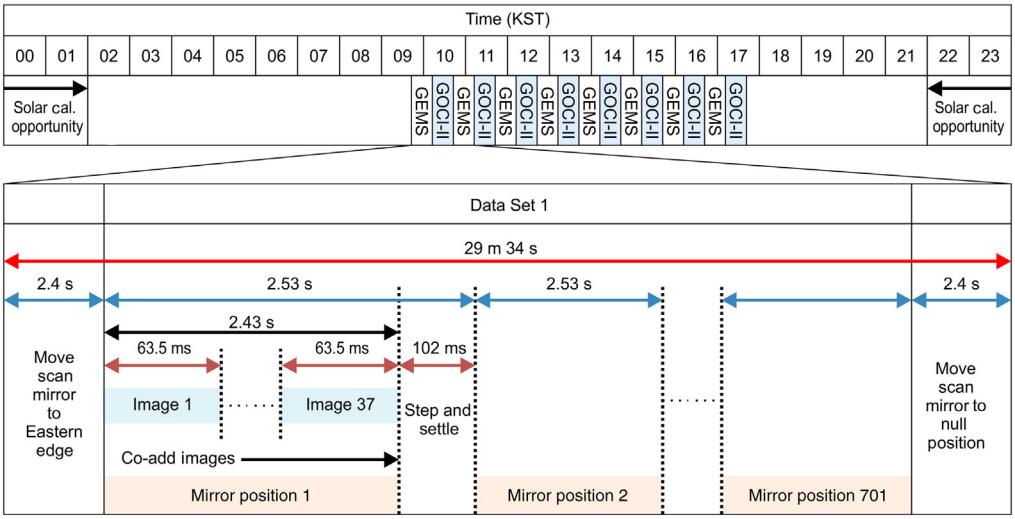

Fig. 3 Basic concept of GEMS operations.

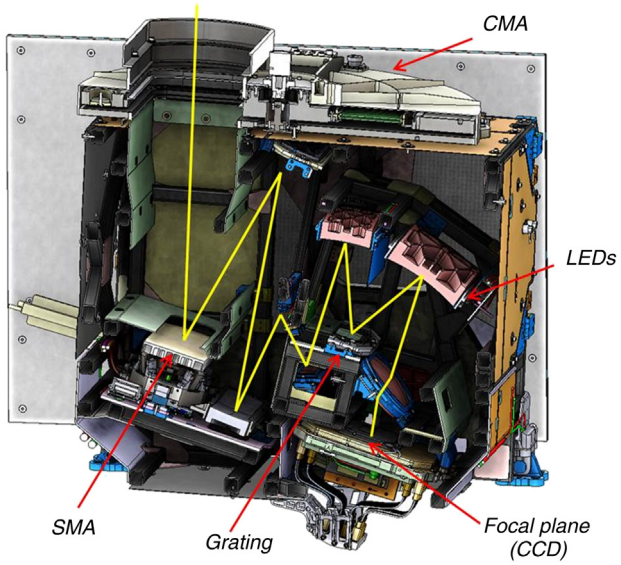

Fig. 4 Optomechanical subsystem of the GEMS.

control after each observation. Spatial coaddings are performed based on product category to enhance the SNR at the ground station, the Environmental Satellite Center (ESC), which eventually improves the accuracy of the level 2 data.

3.2 *Spectral Performance*

The GEMS bandpass function has been measured at selected wavelengths (Table 3). Using a laser with an accuracy of 0.006 nm, 10 images were captured at each wavelength with a sampling interval of 0.06 nm over the scan range of ± 1.8 nm. The collected data were used to determine bandpass function with the wavelengths for the maximum bandpass as well as for the FWHM. The point spread function (PSF) was calculated at four selected wavelengths (300, 370, 430, and 500 nm) and three spatial positions. The PSF was characterized at the spectroscopic level.

Signals at both extremes of the bandpass function are hidden by noise, making them difficult to measure. Thus, broadband characterization was performed with multiple laser sources and long pass filters. These data can also be utilized in the assessment of stray light performance with the PSF. Stray light can be also from out-of-band (i.e., wavelengths outside of 300 to

Table 3 Spectral scale and bandpass test matrix.

Spectral scale center wavelength	Bandpass wavelength scan range (from center)	Bandpass wavelength sampling interval (step size)	Number of samples per wavelength
301.8	±1.8 nm	0.06 nm	10 images
330.0			
365.0			
400.0			
435.0			
470.0			
498.2			

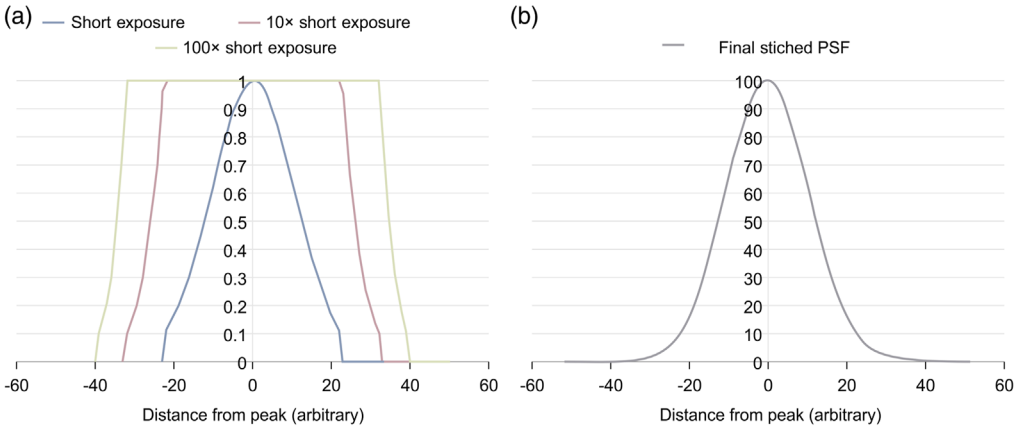

Fig. 5 PSF results using the "stitching method": (a) before PSF and (b) after PSF.

500 nm) and out-of-field, which is spatially affected in the north–south direction. To measure stray light, data from the middle range are collected using a proper laser source intensity (or exposure length) level to ensure that signals at middle wavelengths (370 and 430 nm) are not saturated. Even if the signal in the middle range becomes saturated, the laser source intensity can be set so that data from the two extremes are greater than the noise level and can be subsequently recorded with high SNRs. Similarly, ranges at the extremes can also be analyzed with high SNRs by using a stronger laser source. As shown in Fig. 5, a clean PSF without the influence of noise can be obtained by standardizing collected data to their corresponding laser source intensities.

As opposed to methods involving adjustment of light source intensity, GEMS collects data by adjusting the laser exposure time. This method ensures uniformity of the laser source with respect to wavelength and makes standardization easier. In addition, adjusting the laser exposure time is more accurate than adjusting the intensity of the laser source.

3.3 *Calibration*

GEMS covers a wavelength range of 200 nm (between 300 and 500 nm) with a spectral resolution of 0.6 nm; the accuracy of the final output is heavily affected by the slightest perturbations in the observations. Hence, GEMS is expected to validate and calibrate its observational data through methods such as solar observation and light-emitting diode (LED)-assisted linearity analysis. Representative on-orbit calibration activities include solar observations using diffusers of GEMS, dark imaging with the calibration wheel in closed position, utilization of internal LEDs, and the validation of linearity of the results (Table 4).

Table 4 Radiometric calibration activities.

Radiometric calibration activity	Frequency	Time
Dark imaging	Two times/day	Before and after daytime recording
Working solar diffuser observation	One time/day	Before midnight; solar elevation angle at 30 deg
Internal LED observation	One time/week	Between dark imaging and solar diffuser observation
Reference solar diffuser observation	Two times/year	Before midnight; solar elevation angle at 30 deg

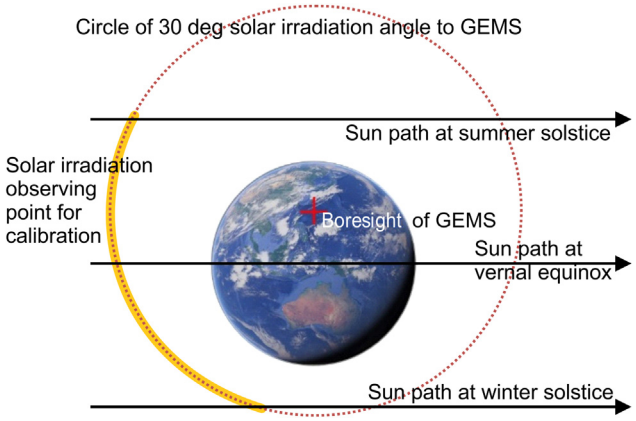

Fig. 6 Solar calibration geometry over a yearly cycle.

3.3.1 *Working/reference diffuser calibration*

GEMS monitors the Sun once a day to validate and calibrate any self-caused changes in the Earth's radiance data. For this reason, GEMS is equipped with a calibration mechanism assembly (CMA), which has an open position for Earth observations, two diffuser positions, and a closed position to prevent incoming debris. GEMS also carries a working diffuser as well as a reference diffuser to correct the degradation of the working diffuser every 6 months. The diffuser is used for solar calibrations before midnight when the incident angle of sunlight on GEMS is ~30 deg. The diffuser transmission is affected by the solar incidence angle; thus, the solar calibration time during the year is determined at a constant incident angle (Fig. 6).

Observed solar irradiance $[F_{\text{meas}}(i,j)]$ is used to calibrate the Earth radiance observations from GEMS compared to existing reference values. $F_{\text{meas}}(i,j)$ is expressed as

$$F_{\text{meas}}(i,j) = \frac{k^r_{i,j} \cdot C^i_{\text{photon}}(i,j)}{\text{BTDF}_{\text{Diffuser}}(G_{i,j}) \cdot N_{\text{Coadd}} \cdot t_{\text{int}}}, \tag{2}$$

where $k^r_{i,j}$ is the pixel radiance calibration coefficient at column i, row j; $C^i_{\text{photon}}(i,j)$ is the measured signal in irradiance mode at column i, row j; $\text{BTDF}_{\text{Diffuser}}(G_{i,j})$ is the bidirectional transmission distribution function (BTDF) of the on-board diffuser, which is a function of the goniometric angle; N_{Coadd} is the number of image coadditions; and t_{int} is the single frame integration time.

3.3.2 *Dark imaging and on-board LED source linearity calibration*

Dark imaging is performed to analyze GEMS noise signals and to offset values when the CMA is in the closed position. The imaging is conducted twice daily (before and after Earth observations) and is used for the current dark correction during the observation. Dark calibration is performed

by combining the frames of dark imaging and normal observation, which have the same integration times and numbers of images.

In addition, GEMS utilizes its internal LEDs once a week to check the homogeneity of CCDs and the linearity of the image. It collects LED images at 20 different times and interpolation is used in between. Each data element consists of a combination of five frames. The calibration wheel moves to the closed position during LED imaging.

4 Main Products

GEMS is expected to provide a total of 16 level 2 (L2) products (Table 5), including aerosol optical depth (AOD), ozone (O_3), and trace gases in the atmosphere such as sulfur dioxide (SO_2), nitrogen dioxide (NO_2), glyoxal (CHOCHO), and formaldehyde (HCHO).

Some GEMS products are provided as vertical column densities (VCD) by retrieving slant column densities and applying the air mass factor (AMF). The acquired data are expected to be used as feedback for the detection of clear sky pixels and calculation of surface reflectance to further contribute to the improvement of accuracy. The accuracy of the products retrieved is needed to be validated after the satellite launched.

4.1 *Aerosol Optical Depth*

Aerosols affect the human body via respiration: they are deposited in the bronchial tract, often reaching the lungs, where they critically endanger health by accumulating in the cardiovascular system. Aerosols can even create economic losses by damaging precision industries. Owing to their detrimental health effects, the World Health Organization (WHO) has classified PM as group 1 carcinogens.[1] Not only does the absorption and scattering of solar energy used by aerosols have a direct and critical effect on global climate change,[26–28] indirect meteorological effects are also caused by physical processes related to clouds and precipitation.

While radiative energy in the 300- to 500-nm range is only slightly affected by the ground surface, it is strongly affected by air molecule scattering and the absorption/scattering effects of aerosols, making it useful in aerosol-type determinations or optical depth calculations. The GEMS AOD output algorithm uses a radiative transfer model to calculate a lookup table (LUT) and estimate the AOD by applying an inversion method to compare top-of-atmosphere reflectance and the LUT data. The AOD is very sensitive to clouds; therefore, only clear regions without any clouds are selectively used for calculations. The accuracy of data is determined by the cloud detection accuracy as well as the spectral properties and size distribution of the aerosols used in the LUT. The temporal resolution of the AOD output is identical to the temporal resolution of the general observation and calculations can be performed on a single pixel of the spatial resolution mentioned in Sec. 2.1 (3.5×8 km per pixel based on the Seoul area).

Table 5 Main L2 outputs of the GEMS unit.

No.	Output	No.	Output
1	NO_2 VCD (molecular number/cm^2)	9	Aerosol optical depth
2	SO_2 VCD (molecular number/cm^2)	10	Aerosol index
3	HCHO VCD (molecular number/cm^2)	11	Single scattering albedo
4	CHOCHO VCD (molecular number/cm^2)	12	Aerosol height (km)
5	O_3 VCD (molecular number/cm^2)	13	Cloud pressure (hPa)
6	O_3 stratosphere density (molecular number/cm^2)	14	Impactive cloud fraction
7	Upper troposphere O_3 density (molecular number/cm^2)	15	Surface reflectivity
8	Lower troposphere O_3 density (molecular number/cm^2)	16	UV index

4.2 *Ozone*

Ozone is a trace gas composing 0.001% of atmospheric volume. It is a short-lived climate pollutant (SLCP) and its contribution to the greenhouse effect closely follows that of carbon dioxide (CO_2) and methane (CH_4).[29] Moreover, although stratospheric O_3 absorbs ultraviolet rays from the sun and creates a viable environment on the Earth's surface, tropospheric O_3 is a key secondary pollutant that is detrimental to the human body and various ecosystems. With recent rapid economic growth in East Asia and the subsequent increase in fossil fuel consumption, a significant volume of air pollutants is emitted and the amount of the secondary pollutant O_3 is increasing, creating concerns for human health and ecological damage.[30–32]

The GEMS O_3 calculation algorithm outputs total O_3 and a vertical profile, where the wavelength range for the calculation of accumulated tropospheric O_3 concentrations is 300 to 340 nm. Tropospheric O_3 can be calculated with low analytical error using signals in the ultraviolet range at the ground level. The calculation algorithm utilizes a nonlinear optimal estimation to minimize the difference between measured and simulated spectral radiances and the difference between retrieved and *a priori* state vectors, constrained with measurement and a priori error covariance matrices.[33] The accuracy of the final accumulated O_3 concentration is determined by factors such as the measured satellite signal accuracy and the O_3 sensitivity dependent on vertical height, and is calculated over cloudless, clear sky pixels. The temporal resolution is identical to that of the general observation, and calculations of the accumulated O_3 can be performed by coadding two pixels of GEMS spatial resolution (7×8 km).

4.3 *Nitrogen Dioxide and Sulfur Dioxide*

Accumulated NO_2 and SO_2 concentrations are calculated from the GEMS spectral imaging calibration data for 400 to 500 nm and 305 to 320 nm, respectively. Using satellite signals from areas with low amounts of NO_2 or SO_2 as references, the signals of aerosols and air molecules with slow absorption effects are removed. Using the differential optical absorption spectroscopy (DOAS) method,[34] the VCDs are calculated by fitting the gas-specific absorption cross-section data from the database.

The accuracies of the final accumulated NO_2 and SO_2 concentrations are determined from the calculation errors between the AMF and the residual noise signals after the DOAS fitting. The temporal resolution is identical to that of the general observation and calculations of the accumulated NO_2 can be performed by coadding two pixels of GEMS resolution (7×8 km). For the sake of improving the precision and SNR of SO_2, eight pixels of the GEMS resolution are coadded and averaged over up to 3 h.

4.4 *Formaldehyde*

Most of the HCHO in the atmosphere is produced from oxidation of CH_4. High concentrations of HCHO at the ground level can be observed when it is directly released into the atmosphere (e.g., wildfires); however, the main product is isoprene (C_5H_8). The emission of C_5H_8 can be derived from the VCD of HCHO, which can be observed via satellites.[35–41] Satellite observation of HCHO can be a key contributor to the estimation of VOCs over large areas and the reduction of uncertainty.

The accumulated HCHO calculation algorithm of GEMS uses basic optical absorption spectroscopy (BOAS) technology over a wavelength range of 327 to 358 nm. The BOAS technology fits the directly measured satellite radiance signals, numerous variables stored in the library, and the gas-specific absorption cross-section data to calculate the accumulated concentrations of HCHO. The accuracies of the accumulated HCHO concentrations are determined from the calculation errors between the AMF and the residual noise signals after the BOAS fitting.

Calculations for HCHO are performed over clear sky pixels and the temporal resolution is identical to that of the general observation. The calculations of the accumulated HCHO can be performed by coadding eight pixels of the spatial resolution as mentioned in Sec. 2.1 (14×16 km/pixel) and averaged over 3 h.

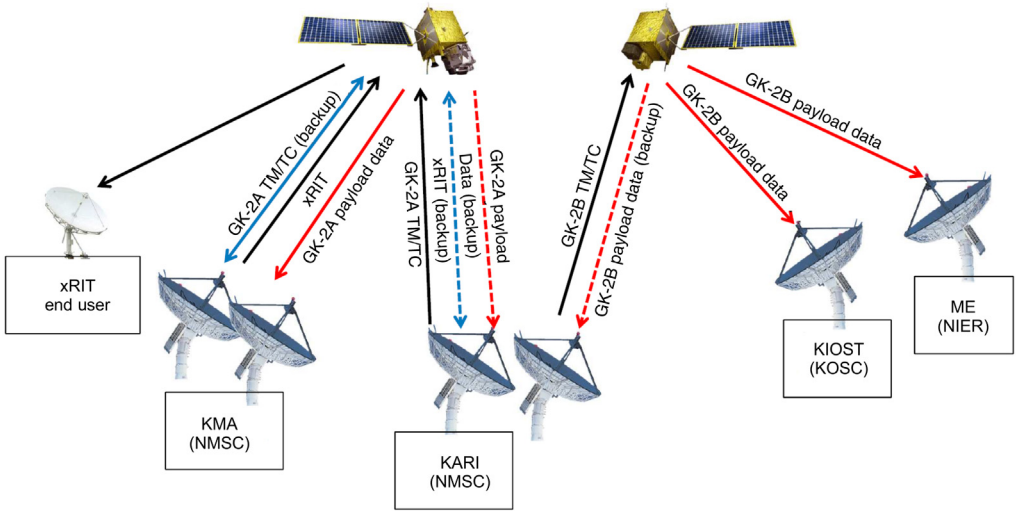

Fig. 7 Systematic diagram of the GK-2 ground control process.

5 GEMS Ground Station

For the reception, processing, and application of GEMS data, the Korean Ministry of Environment constructed the ESC at the NIER and established a data processing system. The NIER is currently conducting an integrated air quality forecast;[42] a significant improvement in the forecast accuracy is expected with the utilization of GEMS data.

GEMS data are simultaneously received at the Korea Aerospace Research Institute, which controls the satellite bus system, and the Korea Ocean Satellite Center, which is the ground control station for the GOCI-II and holds a mutual data backup relationship with its counterparts (Fig. 7). The raw data observed from GEMS and received via the reception system at the ESC produce the L1B data through the decomposition module, radiation calibration, and geometric calibration. The L2 data are provided in the form of outputs such as AOD (Fig. 8 and Table 6). To improve the accuracy of the main L2 outputs at the ESC, forecast data from the ocean color satellite GOCI-II and the atmospheric chemistry modeling data are collected. The production of external-data driven value-added products, including mean field and surface concentrations, is in preparation.

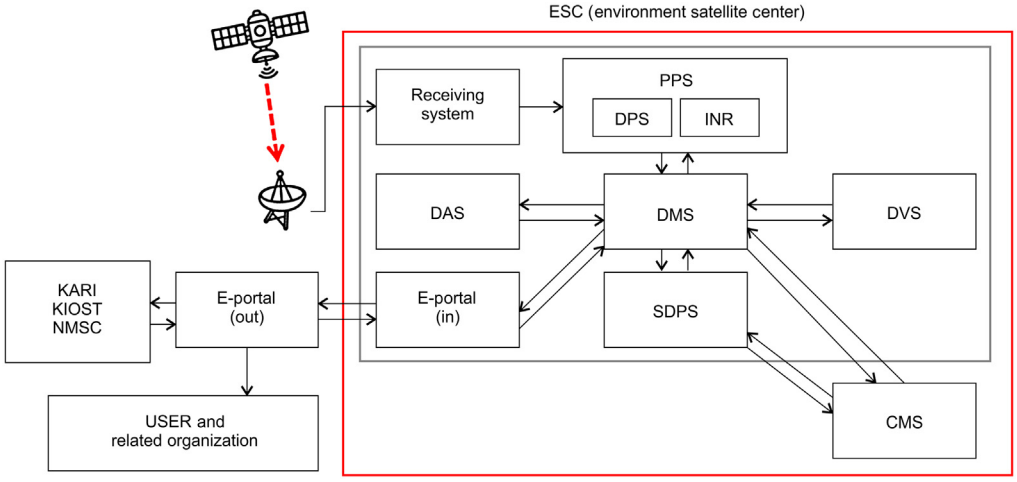

Fig. 8 Structural diagram of the GEMS data processing system.

Table 6 Abbreviations of GEMS data processing systems.

Abbreviation	Explanation
PPS	Data preprocessing system
DAS	Data analysis system
DMS	Data management system
DVS	Data verification system
SDPS	Scientific data processing system
CMS	Control and monitoring system

6 Application and Expected Impacts of GEMS

GEMS is expected to provide the hourly distribution of the product variables and simultaneously analyze their emission, transport, and sinks. Unlike those of LEO environmental satellites, the spatial and temporal distribution characteristics of GEMS enable continuous monitoring of O_3, SO_2, NO_2, aerosols, and HCHO from a single location; it thus has a wide range of expected applications, including top-down pollutant emissions and long-range transport. In particular, it is anticipated that emission calculations and monitoring will be possible through the spatial and temporal observations of tropospheric O_3, PMs, VOCs, and precursors,[43] and that these will be utilized in the quantitative analysis and transport pathway determination of long-range air pollutants. Furthermore, methods to calculate the surface concentrations of PM could be developed using the satellite-observed AODs,[44–47] which would be useful in the monitoring of PM distributions, and analyses of their trends and high PM concentration events.

In the field of climate change, GEMS is expected to contribute toward understanding active climate change responses, such as quantitative analyses related to climate change through the consistent monitoring of surface and atmospheric East Asian SLCP (e.g., O_3, aerosols) concentrations. It is also likely to provide solutions to reduce SLCPs, which, unlike long-lived CO_2, represent short-term reduction effects.

Furthermore, GEMS is anticipated to be used in the detection of sulfuric gases, as an indicator of volcanic eruptions, for the confirmation, prediction, and analysis of air pollutants (e.g., toxic substances), for understanding transport paths from chemical accidents, and the quantitative estimation of air pollutants from large wildfires.

In particular, the use of GEMS as input data in air quality models is expected to significantly improve forecast accuracies through data assimilation and the amelioration of initial and boundary condition uncertainties.[48,49] GEMS may also bring about quality improvement through the evaluation of air quality prediction models, accuracy enhancement of air pollutant emissions through bottom-up estimations, and through accuracy enhancement and improvement of air quality prediction intervals through assimilation of satellite data and forecast models.[49–51] It is also likely to improve the accuracy of air pollution forecasts and warnings through earlier estimation of high air pollutant concentrations. These examples of forecast and warning accuracy improvements will enhance public trust and increase air pollution avoidance rates; thus, improving the health and quality of life of citizens.

Lastly, along with TEMPO[22] and Sentinel-4,[23] GEMS is expected to ensure broad and consistent monitoring of air quality in East Asia, North America, and Europe's concentrated areas. In conjunction with scientific data for air pollutant emissions, transport, and degradation at the global scale, international cooperation among state governments and efficient air quality policy implementation will be achievable. It should be noted that globally spreading air pollution is impossible to mitigate with the efforts of only a few nations. Therefore, the three major geostationary environmental satellites, including GEMS, are anticipated to provide solutions for international cooperation and ensure efficient and effective air quality control.

7 Conclusions

The South Korean government is developing the first geostationary environment spectrometer (GEMS) and planning its launch in 2019 to consistently monitor deteriorating air quality and establish and enforce efficient and cost-effective air quality policies. GEMS is expected to provide fundamental data on trace gases including NO_2, SO_2, HCHO, O_3, and AOD. In addition, its output can be utilized in air quality prediction models and contribute toward increasing the accuracy of forecasts and warnings that are needed to prevent air pollution, thereby enhancing quality of life. Moreover, GEMS will potentially be able to contribute to international efforts and assist in the development of a clean atmosphere.

Acknowledgments

This research was funded by the National Institute of Environment Research (NIER) funded by the Ministry of Environment (MOE) of the Republic of Korea; Award Nos. NIER-2018-01-01-020 and NIER-2018-01-01-022. M. H. Ahn was supported by the Ministry of Environment (MOE) of the Republic of Korea as "Public Technology Program based on Environment Policy (2017000160002)." The authors declare no conflict of interest.

References

1. World Health Organization (WHO), *Health Effects of Particulate Matter: Policy Implications for Countries in Eastern Europe, Caucasus and Central Asia*, World Health Organization Regional Office for Europe, Copenhagen (2013).
2. World Health Organization (WHO), *World Health Statistics 2016: Monitoring Health for the SDGs*, World Health Organization Regional Office for Europe, Copenhagen, 2016, http://www.who.int/gho/publications/world_health_statistics/2016/en/.
3. Organization for Economic Co-operation and Development (OECD), *How's Life? 2015: Measuring Well-Being*, OECD Publishing, Paris (2015).
4. Ministry of Environment, Republic of Korea, *Special Act on the Improvement of Air Quality in Seoul Metropolitan Area*, Ministry of Environment, Republic of Korea (2005).
5. H. Kim, H. Kim, and J. T. Lee, "Effects of ambient air particles on mortality in Seoul: have the effects changed over time?" *Environ. Res.* **140**, 684–690 (2015).
6. K. Vellingiri et al., "Changes in NO_x and O_3 concentrations over a decade at a central urban area of Seoul, Korea," *Atmos. Environ.* **112**, 116–125 (2015).
7. Z. He et al., "Characteristics of PM2.5 species and long-range transport of air masses at Taean background station, South Korea," *Atmos. Environ.* **37**, 219–230 (2003).
8. B. N. Duncan et al., "A space-based, high-resolution view of notable change in urban NO_x pollution around the world (2005–2014)," *J. Geophys. Res. Atmos.* **121**, 976–996 (2016).
9. Y.-S. Koo et al., "The simulation of aerosol transport over East Asia region," *Atmos. Res.* **90**, 264–271 (2008).
10. A. Richter et al., "Increase in tropospheric nitrogen dioxide over China observed from space," *Nature* **437**, 129–132 (2005).
11. E. Saikawa et al., "Present and potential future contributions of sulfate, black and organic carbon aerosols from China to global air quality, premature mortality and radiative forcing," *Atmos. Environ.* **43**, 2814–2822 (2009).
12. C.-H. Kim et al., "Long-term simulations of the sulfur concentrations over the China, Japan and Korea: a model comparison study," *Asia-Pac. J. Atmos. Sci.* **47**, 399–411 (2011).
13. M. Kajino et al., "Source-receptor relationships of nitrate in Northeast Asia and influence of sea salt on the long-range transport of nitrate," *Atmos. Environ.* **79**, 67–78 (2013).
14. S. Park, G.-H. Yu, and S. Lee, "Optical absorption characteristics of brown carbon aerosols during the KORUS-AQ campaign at an urban site," *Atmos. Res.* **203**, 16–27 (2018).
15. H. Kim, Q. Zhang, and J. Heo, "Influence of intense secondary aerosol formation and long-range transport on aerosol chemistry and properties in the Seoul Metropolitan Area during spring time: results from KORUS-AQ," *Atmos. Chem. Phys.* **18**, 7149–7168 (2018).

16. H. Bovensmann et al., "SCIAMACHY: mission objectives and measurement modes," *J. Atmos. Sci.* **56**, 127–150 (1999).
17. P. F. Levelt et al., "The ozone monitoring instrument," *IEEE Trans. Geosci. Remote Sens.* **44**, 1093–1101 (2006).
18. J. P. Veefkind et al., "TROPOMI on ESA sentinel-5 precursor: a GMES mission for global observations of the atmospheric composition for climate, air quality and ozone layer applications," *Remote Sens. Environ.* **120**, 70–83 (2012).
19. R. V. Martin, "Satellite remote sensing of surface air quality," *Atmos. Environ.* **42**, 7823–7843 (2008).
20. P. Ingmann et al., "Requirements for the GMES atmosphere service and ESA's implementation concept: sentinels-4/-5 and -5p," *Remote Sens. Environ.* **120**, 58–69 (2012).
21. D. Goh, "China launches Gaofen-5 hyperspectral imaging satellite for atmospheric research," *SpaceTech Asia*, 2018, http://www.spacetechasia.com.
22. P. Zoogman et al., "Tropospheric emissions: monitoring of pollution (TEMPO)," *J. Quant. Spectrosc. Radiat. Transfer* **186**, 17–39 (2017).
23. G. B. Courrèges-Lacoste et al., "The copernicus sentinel 4 mission: a geostationary imaging UVN spectrometer for air quality monitoring," *Proc. SPIE* **10423**, 1042307 (2017).
24. P. Coste et al., "Development of the new generation of geostationary ocean color imager," *Proc. SPIE* **10562**, 105620D (2017).
25. H. O. Kim et al., "Space-based earth observation activities in South Korea," *IEEE Geosci. Remote Sens.* **3**, 34–39 (2015).
26. M. O. Andrea, C. D. Jones, and P. M. Cox, "Strong present-day aerosol cooling implies a hot future," *Nature* **435**, 1187–1190 (2005).
27. Y. J. Kaufman, D. Tanré, and O. A. Boucher, "A satellite view of aerosols in the climate system," *Nature* **419**, 215–223 (2002).
28. J. Seinfeld, "Atmospheric science: black carbon and brown clouds," *Nat. Geosci.* **1**, 15–16 (2008).
29. S. Solomon et al., "Climate change 2007: the physical science basis," IPCC Report, Cambridge University Press, Cambridge and New York (2007).
30. D. J. Jacob, J. A. Logan, and P. P. Murti, "Effect of rising Asian emissions on surface ozone in the United States," *Geophys. Res. Lett.* **26**, 2175–2178 (1999).
31. D. Jaffe et al., "Transport of Asian air pollution to North America," *Geophys. Res. Lett.* **26**, 711–714 (1999).
32. D. L. Mauzerall et al., "Seasonal characteristics of tropospheric ozone production and mixing ratios over East Asia: a global three-dimensional chemical transport model analysis," *J. Geophys. Res. Atmos.* **105**, 17895–17910 (2000).
33. C. D. Rodgers, *Inverse Methods for Atmospheric Sounding: Theory and Practice*, World Scientific Publishing Co. Pte. Ltd., Singapore (2000).
34. U. Platt and D. Perner, "Direct measurements of atmospheric CH_2O, HNO_2, O_3, NO_2, and SO_2 by differential optical absorption in the near UV," *J. Geophys. Res. Oceans* **85**, 7453–7458 (1980).
35. D. S. Abbot et al., "Seasonal and interannual variability of North American isoprene emissions as determined by formaldehyde column measurements from space," *Geophys. Res. Lett.* **30**(17) (2003).
36. M. P. Barkley et al., "Top-down isoprene emissions over tropical south America inferred from SCIAMACHY and OMI formaldehyde columns," *J. Geophys. Res. Atmos.* **118**, 6849–6868 (2013).
37. T. M. Fu et al., "Space-based formaldehyde measurements as constraints on volatile organic compound emissions in east and south Asia and implications for ozone," *J. Geophys. Res. Atmos.* **112**, D06312 (2007).
38. P. I. Palmer et al., "Mapping isoprene emissions over North America using formaldehyde column observations from space," *J. Geophys. Res. Atmos.* **108**, 4180 (2003).
39. P. I. Palmer et al., "Quantifying the seasonal and interannual variability of North American isoprene emissions using satellite observations of the formaldehyde column," *J. Geophys. Res. Atmos.* **111**, D12315 (2006).

40. T. Stavrakou et al., "Isoprene emissions over Asia 1979–2012: impact of climate and land-use changes," *Atmos. Chem. Phys.* **14**, 4587–4605 (2014).
41. K. Chance et al., "Satellite observations of formaldehyde over North America from GOME," *Geophys. Res. Lett.* **27**, 3461–3464 (2000).
42. L. S. Chang et al., "Human-model hybrid Korean air quality forecasting system," *J. Air Waste Manage. Assoc.* **66**, 896–911 (2016).
43. A. Van Donkelaar et al., "Analysis of aircraft and satellite measurements from the Intercontinental Chemical Transport Experiment (INTEX-B) to quantify long-range transport of East Asian sulfur to Canada," *Atmos. Chem. Phys.* **8**, 2999–3014 (2008).
44. Z. Ma et al., "Satellite-based spatiotemporal trends in $PM_{2.5}$ concentrations: China 2004–2013," *Environ. Health Perspect.* **124**, 184–192 (2016).
45. J. W. Xu et al., "Estimating ground-level $PM_{2.5}$ in eastern China using aerosol optical depth determined from the GOCI satellite instrument," *Atmos. Chem. Phys.* **15**, 13133–13144 (2015).
46. W. You et al., "Estimating $PM_{2.5}$ in Xi'an, China using aerosol optical depth: a comparison between the MODIS and MISR retrieval models," *Sci. Total Environ.* **505**, 1156–1165 (2015).
47. S. Seo et al., "Estimation of PM_{10} concentrations over Seoul using multiple empirical models with AERONET and MODIS data collected during the DRAGON-Asia campaign," *Atmos. Chem. Phys.* **15**, 319–334 (2015).
48. Y. Liu, C. J. Paciorek, and P. Koutrakis, "Estimating regional spatial and temporal variability of $PM_{2.5}$ concentrations using satellite data, meteorology, and land use information," *Environ. Health Perspect.* **117**, 886–892 (2009).
49. P. E. Saide et al., "Assimilation of next generation geostationary aerosol optical depth retrievals to improve air quality simulations," *Geophys. Res. Lett.* **41**, 9188–9196 (2014).
50. M. E. Park et al., "New approach to monitor transboundary particulate pollution over Northeast Asia," *Atmos. Chem. Phys.* **14**, 659–674 (2014).
51. M. Sofiev et al., "An operational system for the assimilation of the satellite information on wild-land fires for the needs of air quality modeling and forecasting," *Atmos. Chem. Phys.* **9**, 6833–6847 (2009).

Won Jun Choi is a researcher at the National Institute of Environmental Research (NIER). He is working on the overall project for air quality monitoring using GEMS from the beginning to the present, and contributed to making the air quality monitoring plan using space technologies in the environmental field.

Kyung-Jung Moon is a researcher at the NIER. He has been conducting research on the integration and evaluation the GEMS algorithm, and he is working on transforming the integrated algorithms for calculation air quality system using GEMS radiation data.

Jongmin Yoon is a senior researcher at the NIER. He is a middle manager of development for algorithms to calculate the concentration of trace gas using GEMS spectral data in real time, and also of data processing system development.

Ara Cho is a researcher at the NIER. She is developing data processing system of environmental satellite center (ESC). She is studying in the long-range transboundary of air pollutants using satellite data.

Sang-kyun Kim is the director of ESC at the NIER, which oversees the development of GEMS and is responsible for the satellite work in the field of atmospheric environment including GEMS. He is doing the effort to expand the use of environmental satellites, such as the calculation of surface concentration using satellite observations and monitoring of atmospheric sources.

Seounghoon Lee is a senior researcher at Korea Aerospace Research Institute (KARI). He is a principal investigator of development and manufacturing for GEMS hardware which will be loaded on GeoKOMPSAT2B (GK2B). Optical observation equipment mounted on multiple satellites was developed under his responsibility.

Dai ho Ko is a researcher at KARI. He is responsible for the development and production of GEMS, including the development of preprocessing algorithms for GEMS. He is also involved in the development of optical equipment for satellites.

Jhoon Kim is a professor at Yonsei University. He is responsible for the aerosol optical depth calculating algorithm from GEMS spectral data, and the project manager (PM) of GEMS level 2 (L2) algorithms development group. He is the centerpiece of the international GEMS science team.

Myung Hwan Ahn is a professor at Ewha Womans University, and a member of the GEMS algorithm research group. He is in charge of developing the GEMS spectral calibration algorithm which corrects the spectral errors that may occur depending on the GEMS hardware characteristics and improves the accuracy of level 2 (L2) algorithm calculation.

Deok-Rae Kim is a researcher at the NIER. He supported the research to evaluate and improve the algorithms developed by the GEMS L2 algorithm development group.

Sang-Min Kim is a researcher at the NIER. He is studying the extraction of surface level from the vertical column density which are the satellites data.

Ji-Young Kim is a senior researcher at the NIER. She was a middle manager in the midstage of the GEMS project, and now she is responsible for joint research on long-range transboundary air pollutants in Korea, China, and Japan.

Dennis Nicks is a PM at Ball Aerospace Technologies Cooperation (BATC). BATC is joint-developing with KARI for GEMS, and he is in charge of BATC.

Jeong-Su Kim is the director general of the Climate and Air Quality Research Department of the NIER. He is in charge of who oversees the study of the atmospheric environment, such as air quality forecasting and atmospheric environment monitoring.